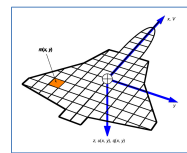
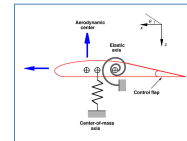


# Aeroelasticity and Fuel Slosh

Robert Stengel, Aircraft Flight Dynamics  
MAE 331, 2018

## Learning Objectives

- Aerodynamic effects of bending and torsion
- Modifications to aerodynamic coefficients
- Dynamic coupling
- Fuel shift and sloshing dynamics



*Flight Dynamics*  
418-419, 549-569, 665-678  
*Airplane Stability and Control*  
Chapter 19

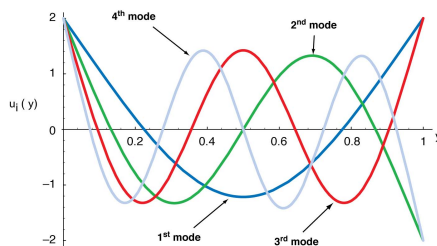
Copyright 2018 by Robert Stengel. All rights reserved. For educational use only.  
<http://www.princeton.edu/~stengel/MAE331.html>  
<http://www.princeton.edu/~stengel/FlightDynamics.html>

## Bending Vibrations of a Free-Free Uniform Beam

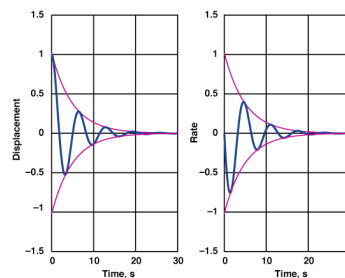
$$EI_y \frac{d^4 z}{dx^4} = k_i = -m' \frac{d^2 z}{dt^2}$$

- In figure, ( $u = z, y = x$ )
- Left side determines vibrational mode shape
- Right side describes oscillation
- Natural frequency of each mode proportional to  $(k_i)^{1/2}$

Mode shapes of bending vibrations



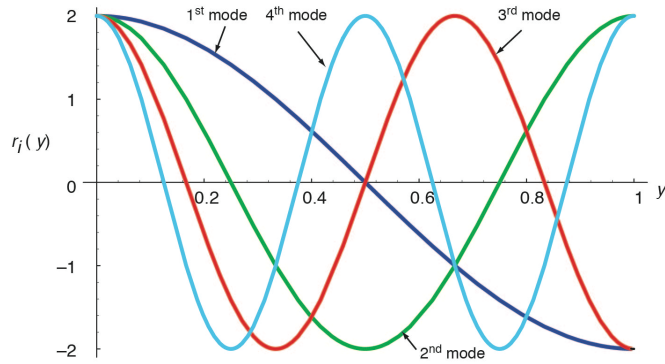
Time response of single mode



## Torsional Vibrations of a Free-Free Uniform Beam

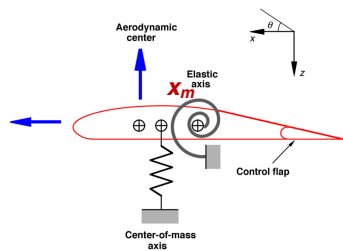
$$GJ \theta'' \Big|_{y=y_s} = I'_{yy} \ddot{\theta} \Big|_{y=y_s}$$

**Mode shapes of torsional vibrations**



3

## One-Dimensional Model of Wing Aeroelasticity



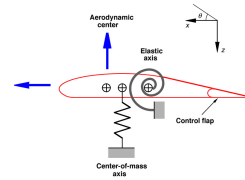
- Wing cross section
- $z$  due to bending,  $\theta$  due to torsion
- $m'$  = mass per unit length
- $I'_{yy}$  = inertia per unit length
- $k, c$  = spring constants
- $x_m$  = axis offset
- Aircraft motion neglected
- 4<sup>th</sup>-order system

$$kz = -m' \ddot{z} - x_m m' \ddot{\theta} - \left[ \frac{\partial C_L}{\partial \alpha} (\dot{z}/V + \theta) + \frac{\partial C_L}{\partial \delta} \delta \right] \bar{q} \bar{c}$$

$$-c\theta = I'_{yy} \ddot{\theta} + x_m m' \ddot{z} - \left[ \frac{\partial C_m}{\partial \alpha} (\dot{z}/V + \theta) + \frac{\partial C_m}{\partial q} \dot{\theta} + \frac{\partial C_m}{\partial \delta} \delta \right] \bar{q} \bar{c}^2$$

4

# One-Dimensional Model of Wing Aeroelasticity



$$\begin{bmatrix} \Delta \dot{\mathbf{x}}_{bending} \\ \Delta \dot{\mathbf{x}}_{torsion} \end{bmatrix} = \begin{bmatrix} \mathbf{F}_{bending} & \mathbf{F}_{torsion}^{bending} \\ \mathbf{F}_{bending}^{torsion} & \mathbf{F}_{torsion} \end{bmatrix} \begin{bmatrix} \Delta \mathbf{x}_{bending} \\ \Delta \mathbf{x}_{torsion} \end{bmatrix} + \dots$$

$$\begin{bmatrix} \Delta \mathbf{x}_{bending} \\ \Delta \mathbf{x}_{torsion} \end{bmatrix} = \begin{bmatrix} \Delta z \\ \Delta \dot{z} \\ \Delta \theta \\ \Delta \dot{\theta} \end{bmatrix}$$

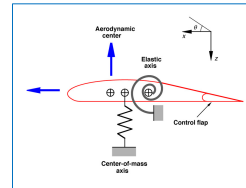
$$\Delta(s) = (s^2 + 2\zeta\omega_n s + \omega_n^2)_{bending} (s^2 + 2\zeta\omega_n s + \omega_n^2)_{torsion}$$

If  $\mathbf{x}_m = \mathbf{0}$

$$\begin{bmatrix} \Delta \dot{\mathbf{x}}_{bending} \\ \Delta \dot{\mathbf{x}}_{torsion} \end{bmatrix} = \begin{bmatrix} \mathbf{F}_{bending} & \mathbf{0} \\ \mathbf{0} & \mathbf{F}_{torsion} \end{bmatrix} \begin{bmatrix} \Delta \mathbf{x}_{bending} \\ \Delta \mathbf{x}_{torsion} \end{bmatrix} + \dots$$

5

# Torsional Divergence



$$\Delta_{torsion}(s) = (s^2 + 2\zeta\omega_n s + \omega_n^2)_{torsion}$$

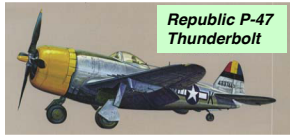
$$x_{aero} \approx \text{quarter chord}; \quad x_{elastic} \approx \text{half chord}; \quad \therefore \partial C_m / \partial \alpha > 0$$

$$\text{If } (\omega_n^2)_{torsion} = \sqrt{\left[ c - \frac{\partial C_m}{\partial \alpha} \left( \frac{\rho \bar{c}^2}{2} \right) V^2 \right] / I'_{yy}} < 0,$$

two real roots, and **one is unstable**

$$V_{torsional \ divergence} = c / \left( \frac{\partial C_m}{\partial \alpha} \left( \frac{\rho \bar{c}^2}{2} \right) \right)$$

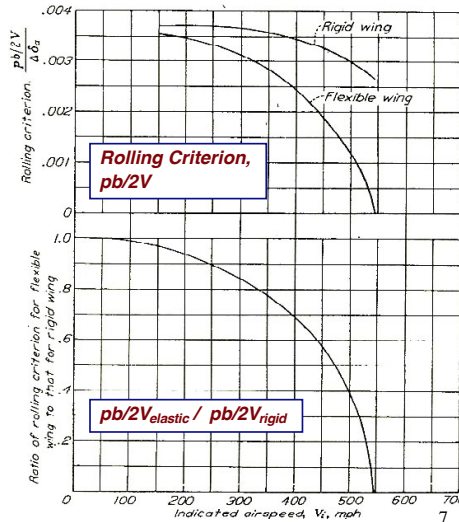
6



Republic P-47 Thunderbolt

## Reduced Aileron Effect Due to Aeroelasticity

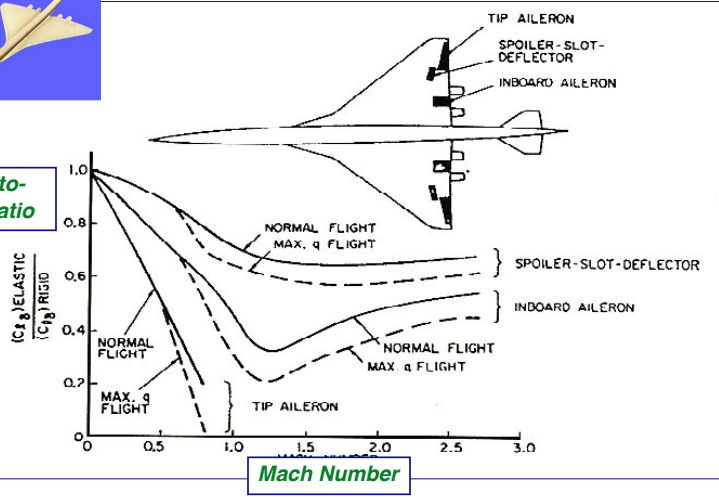
- Wing torsion reduces aileron effect with increasing dynamic pressure



## Aeroelastic Aileron Effect of Boeing 2707-300 Supersonic Transport Concept



Elastic-to-Rigid Ratio



8



## Quasi-Static Aeroelastic Model of Aircraft Dynamics: Residualization

- IF elastic modes are fast compared to rigid modes and are stable

$$\begin{bmatrix} \Delta \dot{\mathbf{x}}_{\text{aircraft}} \\ \mathbf{0} \end{bmatrix} \approx \begin{bmatrix} \mathbf{F}_{\text{aircraft}} & \mathbf{F}_{\text{elastic}}^{\text{aircraft}} \\ \mathbf{F}_{\text{aircraft}}^{\text{elastic}} & \mathbf{F}_{\text{elastic}} \end{bmatrix} \begin{bmatrix} \Delta \mathbf{x}_{\text{aircraft}} \\ \Delta \mathbf{x}_{\text{elastic}} \end{bmatrix} + \begin{bmatrix} \mathbf{G}_{\text{aircraft}} \\ \mathbf{G}_{\text{elastic}} \end{bmatrix} \Delta \mathbf{u}_{\text{aircraft}}$$

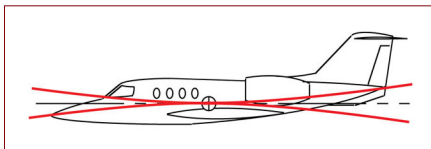
- Residualization reduces aeroelastic model order to rigid-body model order

$$\begin{aligned} \Delta \dot{\mathbf{x}}_a &= \mathbf{F}_a \Delta \mathbf{x}_a - \mathbf{F}_e^a \mathbf{F}_e^{-1} [\mathbf{F}_a^e \Delta \mathbf{x}_a + \mathbf{G}_e \Delta \mathbf{u}_a] + \mathbf{G}_a \Delta \mathbf{u}_a \\ &= \mathbf{F}'_a \Delta \mathbf{x}_a + \mathbf{G}'_a \Delta \mathbf{u}_a \end{aligned}$$

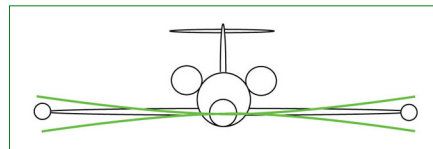
9

## Primary Longitudinal Aeroelastic Mode Shapes

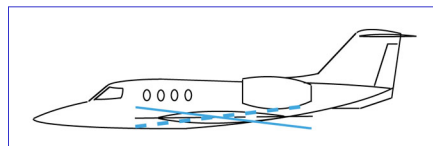
Fuselage Bending



Wing Bending



Wing Torsion



10

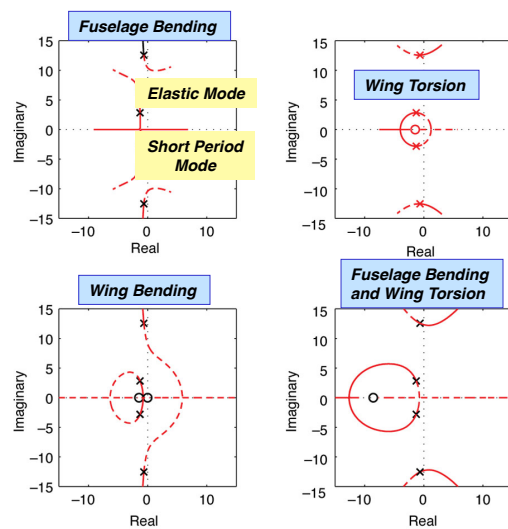
## Aeroelastic Model of Aircraft Dynamics

- Coupled model of rigid-body and elastic dynamics

$$\begin{bmatrix} \Delta \dot{\mathbf{x}}_{aircraft} \\ \Delta \dot{\mathbf{x}}_{elastic} \end{bmatrix} = \begin{bmatrix} \mathbf{F}_{aircraft} & \mathbf{F}_{aircraft}^{elastic} \\ \mathbf{F}_{aircraft}^{elastic} & \mathbf{F}_{elastic} \end{bmatrix} \begin{bmatrix} \Delta \mathbf{x}_{aircraft} \\ \Delta \mathbf{x}_{elastic} \end{bmatrix} + \begin{bmatrix} \mathbf{G}_{aircraft} \\ \mathbf{G}_{elastic} \end{bmatrix} \Delta \mathbf{u}_{aircraft}$$

11

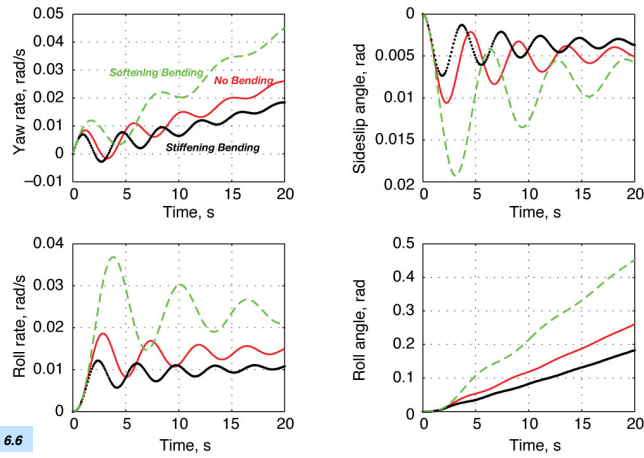
## Effect of Increasing Coupling of Single Aeroelastic Mode with Short Period Roots



Flight Dynamics, 5.6

12

## Effects of Fuselage Aeroelasticity on Lateral-Directional Response to Rudder Step Input

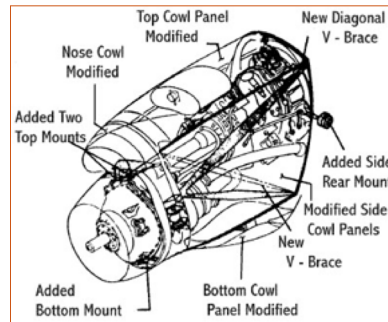
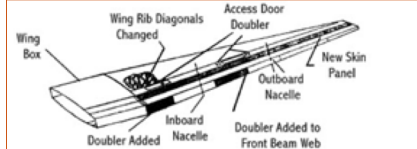


Flight Dynamics, 6.6

13

## Aeroelastic Problems of the Lockheed Electra

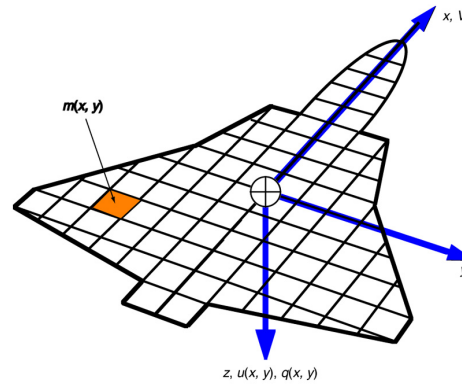
- **Prop-whirl flutter**, 2 fatal accidents (1959-60)
- **Structural modifications made; aircraft remained in service until 1992**
- **Predecessor of US Navy Orion P-3, still in service**



<http://www.youtube.com/watch?v=d0fFNWANK5M>

14

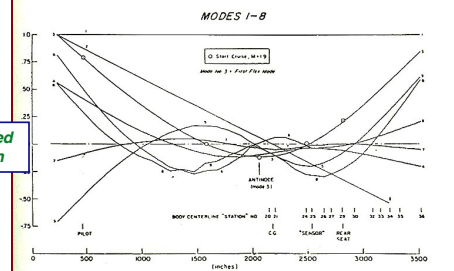
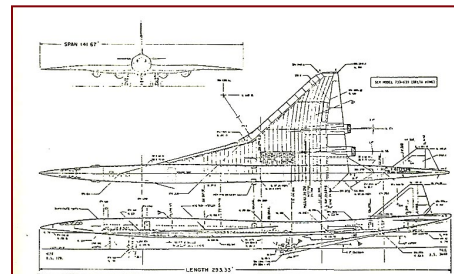
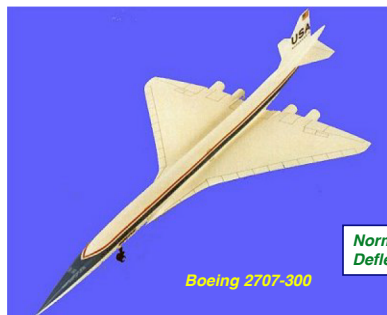
## Two-Dimensional Model of Aeroelastic Airplane



Section 4.6, *Flight Dynamics*

15

## Longitudinal Structural Modes of Boeing 2707-300 Supersonic Transport Concept



Centerline station

16

## Vibrational Mode Shapes for the X-30 (NASP) Vehicle



### Computational Grid for Finite-Element Model

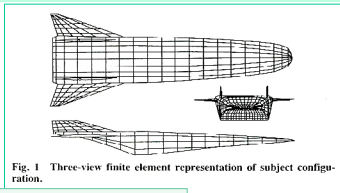


Fig. 1 Three-view finite element representation of subject configuration.

Raney, J. Aircraft, 1995

### Shapes of the First Seven Modes

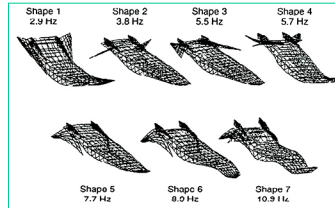


Fig. 2 Structural mode shapes and in-vacuo frequencies included in the aeroelastic model.

**Body elastic deflection distorts the shape of  
scramjet inlet and exhaust ramps**  
**Aeroelastic-propulsive interactions**  
**Impact on flight dynamics**

17

## B-1 Canards for Ride Control

- Elastic modes cause severe, high-g cockpit vibration during low-altitude, high-speed flight
- Active canard surfaces reduce amplitude of the oscillations



18

## Ultra-Light Aircraft

- Extreme aeroelasticity
- *AeroVironment Pathfinder, Centurion, PathfinderPlus* (solar-electric)
- *Helios* in turbulence



**Helios Solar Powered Aircraft**  
 Experiencing turbulence after taking off on first solar powered flight  
 July 14, 2001  
 Dryden Flight Research Center



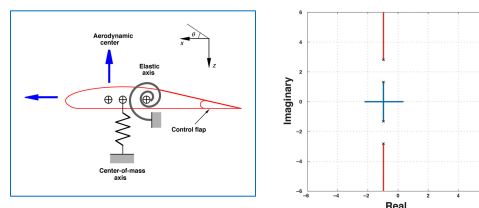
19

## Flutter

If  $x_m \neq 0$

$$\begin{bmatrix} \Delta \dot{x}_{bending} \\ \Delta \dot{x}_{torsion} \end{bmatrix} = \begin{bmatrix} \mathbf{F}_{bending} & \mathbf{F}_{torsion}^{bending} \\ \mathbf{F}_{bending}^{torsion} & \mathbf{F}_{torsion} \end{bmatrix} \begin{bmatrix} \Delta x_{bending} \\ \Delta x_{torsion} \end{bmatrix} + \dots$$

- With increasing  $x_m$ , total damping  $\sim$  constant but redistributed between modes



- ... plus velocity, air density, nonlinear effects, e.g., cubic spring, damping, ...

20



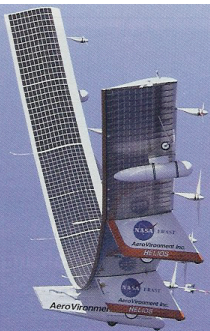
## Aeroelastic Oscillations



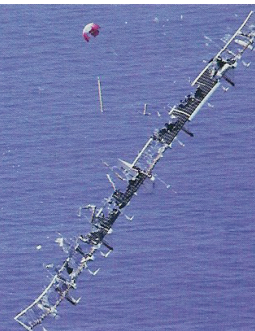
## The Last Flight of *Helios*

- June 6, 2003
- 2,320 lb., 247-ft wingspan, 72 control surfaces, differential thrust
- Change in weight distribution
- 40-ft tip deflection
- **Divergent pitch oscillations**, doubling every 8 seconds
- **Airspeed > 2.5 x limit**

Extreme dihedral occurred before disintegration. It caused pitch instability due to increased pitch inertia and large displacement of center of pressure from center of mass. Tendency to stay at high dihedral was promoted by heavy 520-lb. pod added to the center (long white pod at bottom), along with flight control and structural characteristics. White 165-lb. hydrogen tank cylinder is near tip.



Helios disintegration began near the right wingtip, then spread rapidly as wing skin and solar cells tore off. Pitch oscillation brought airspeed to 2.5 times the design limit.

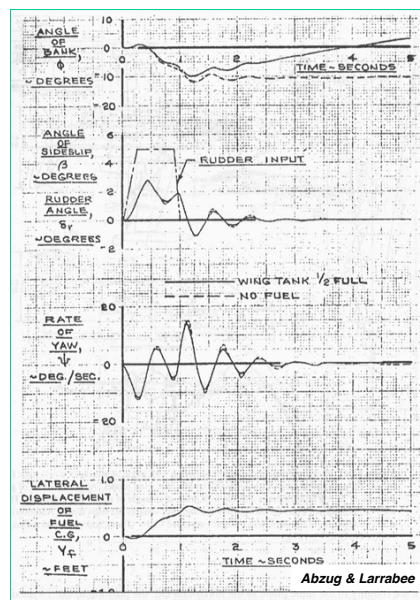
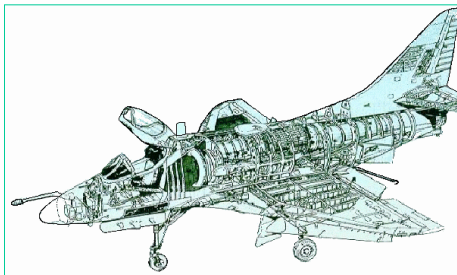


# Fuel Shift and Slosh

23

## Fuel Shift

- Problem with *partially filled fuel tank*
- Single wing tank from tip to tip (A4D)
- Slow, quasi-static shift of fuel c. m.
- Rudder step throws fuel to one side, producing a strong rolling moment

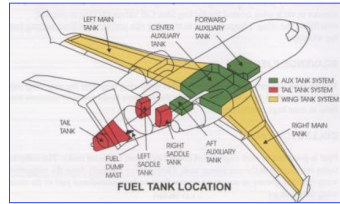


24

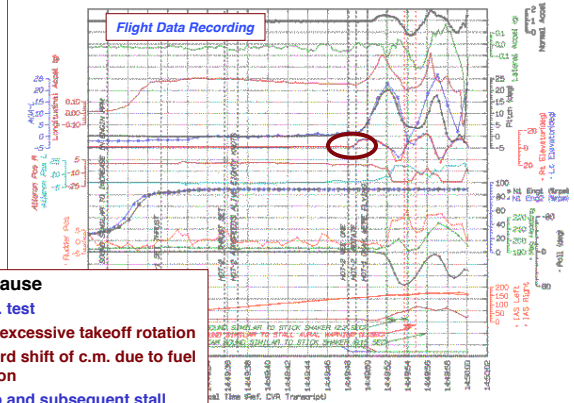


# Fuel Shift

- NTSB/AAB-04/01
- Loss of Control and Impact with Terrain
- Canadair Challenger CL-604 Flight Test Airplane, C-FTBZ
- Wichita, Kansas, October 10, 2000



Angle of Attack



Normal Acceleration

Pitch Angle  
Elevator Angle

IAS  
Altitude

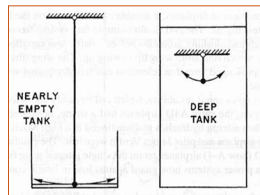
- Probable Cause
  - Aft c.m. test
  - Pilot's excessive takeoff rotation
  - Rearward shift of c.m. due to fuel migration
  - Pitchup and subsequent stall
  - Inadequate test planning

<http://www.nts.gov/investigations/fulltext/aab0401.html>

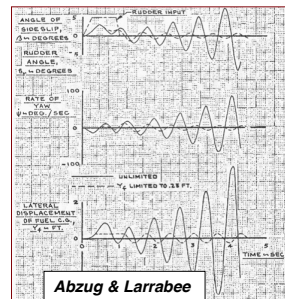
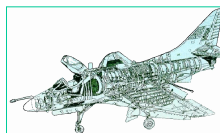
25

# Fuel Slosh

- Dynamic oscillation of fuel center of mass, wave motion at the fuel's surface
- Pendulum and spherical-tank analogies
- Problem is greatest when tank is half-full
- Fore-aft slosh in wing-tip tanks coupled with the short period mode (P-80)



- Fuselage tank forward of the aircraft's center of mass (A4D)
  - Yawing motion excites oscillatory slosh that couples with Dutch roll mode

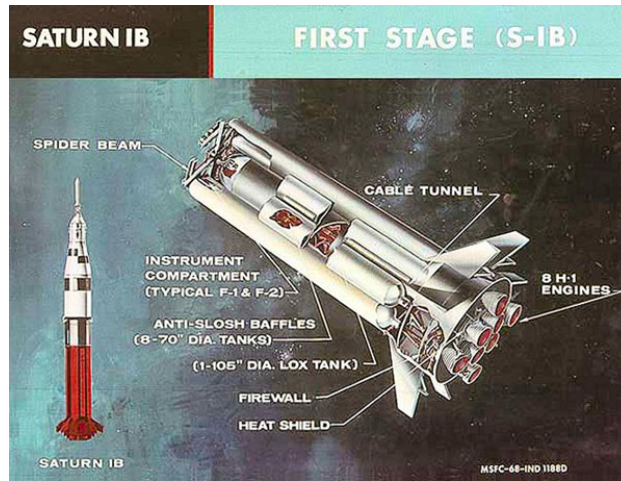


Abzug & Larrabee

26

## Fuel Slosh

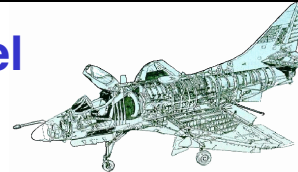
- **Solution: Fuel-tank baffles**
  - Slow down fuel motion
  - Force resonances to higher frequencies due to smaller cavities
  - Wing internal bracing may act as baffle



27



## Problems of Fuel Slosh and Aeroelasticity



- **Coupling of non-rigid dynamic modes with rigid-body modes**
- **Resonant response**
  - Dynamically coupled modes of motion with similar frequencies
  - With light damping, oscillatory amplitudes may become large

$$\begin{bmatrix} \Delta \dot{\mathbf{x}}_{\text{aircraft}} \\ \Delta \dot{\mathbf{x}}_{\text{elastic}} \\ \Delta \dot{\mathbf{x}}_{\text{slosh}} \end{bmatrix} = \begin{bmatrix} \mathbf{F}_{\text{aircraft}} & \mathbf{F}_{\text{elastic}}^{\text{aircraft}} & \mathbf{F}_{\text{slosh}}^{\text{aircraft}} \\ \mathbf{F}_{\text{aircraft}}^{\text{elastic}} & \mathbf{F}_{\text{elastic}} & \mathbf{F}_{\text{slosh}}^{\text{elastic}} \\ \mathbf{F}_{\text{aircraft}}^{\text{slosh}} & \mathbf{F}_{\text{elastic}}^{\text{slosh}} & \mathbf{F}_{\text{slosh}} \end{bmatrix} \begin{bmatrix} \Delta \mathbf{x}_{\text{aircraft}} \\ \Delta \mathbf{x}_{\text{elastic}} \\ \Delta \mathbf{x}_{\text{slosh}} \end{bmatrix} + \mathbf{G} \Delta \mathbf{u}$$

- **Coupling between longitudinal and lateral-directional effects**
- **Nonlinear aerodynamics**
- **Exacerbated by floating control surfaces, high hinge moments, and high aerodynamic angles**

28

## *Next Time: High Speed and Altitude*

*Flight Dynamics*

470-480

*Airplane Stability and Control*

Chapter 11

### **Learning Objectives**

**Effects of air compressibility on flight stability**

**Variable sweep-angle wings**

**Aero-mechanical stability augmentation**

**Altitude/airspeed instability**

29